Journal of Engineering Mathematics **36:** 185–206, 1999.

Optimal fluid injection strategies for *in situ* mineral leaching in two-dimensions

LAWRENCE K. FORBES and SCOTT W. McCUE
Department of Mathematics, University of Queensland, St. Lucia, Queensland 4072, Australia
e-mail: lkf@maths.uq.edu.au

Received 19 November 1997; accepted in revised form 4 December 1998

Abstract. This paper examines the ground-water flow problem associated with the injection and recovery of certain corrosive fluids into mineral bearing rock. The aim is to dissolve the minerals *in situ*, and then recover them in solution. In general, it is not possible to recover all the injected fluid, which is of concern economically and environmentally. However, a new strategy is proposed here, that allows all the leaching fluid to be recovered. A mathematical model of the situation is solved approximately using an asymptotic solution, and exactly using a boundary integral approach. Solutions are shown for two-dimensional flow, which is of some practical interest as it is achievable in old mine tunnels, for example.

Key words: mineral leaching, Darcy's law, boundary-integral approach, injection strategy, withdrawal flows.

1. Introduction

Mineral leaching is a technique for extracting minerals from underground, without using conventional mining techniques of excavation, blasting, crushing and haulage of the ore to the surface for processing. In view of the efficiency of conventional mining operations for high-grade ore deposits, it is unlikely that mineral leaching would be viable in rich ore lodes, but instead, it could be expected to be useful in regions of low ore concentration. The idea is simply to inject a corrosive fluid into the mineral-bearing rock and dissolve some of the mineral, and then to pump out the pregnant liquor through other recovery wells. *In situ* mineral leaching is typically used to extract nonferrous metals such as copper or uranium, and a discussion of the technique may be found in chapter eight of the book by Bartlett [1]. The leaching fluid will be referred to simply as 'acid' in this paper, although it might be a variety of substances, such as sulphuric acid produced from the oxidation of underground pyrites, or ammonium carbonate [1], or dissolved sulphur dioxide [2]. In the case of gold leaching, substances involving cyanides and iodine have been used as lixiviants [3].

Leaching typically occurs in one of two forms. In some cases, mineral-bearing deposits that have been brought to the surface can be irrigated with a corrosive fluid, and the dissolved minerals collected in irrigation channels at ground level. This is referred to as heap leaching or dump leaching, and a model for this situation is given by Pantelis and Ritchie [4], for example. The other situation is the one of interest in the present paper, and involves leaching the ore *in situ*, often deep underground. In this case, access to the ore is obtained by drilling into the rock, pumping in an acid solution under pressure, and then recovering the dissolved mineral through other wells. Several different arrangements of injection and recovery wells are outlined by Bartlett [1].

There are clearly many difficulties associated with the successful operation of an *in situ* mineral leaching facility. Perhaps the most obvious is the environmental danger associated with injecting corrosive liquors deep underground, and the potential for pollution of underground aquifers, for example. Legal restrictions may apply to this type of mining operation, and this is addressed in the article by Crockett [5]. There are also numerous technical difficulties, aside from the practical problems associated with drilling and pumping. It is not an easy matter to determine where injected liquor goes, once it has been pumped into the mineralized rock [6], and this is particularly true if there are cracks or faults in the geology of the site. In addition, it is possible that dynamic changes in the properties of the leached rock can occur during the leaching operation, as a result of the chemical reactions involved. For example, reduced conductivity may result through chemical precipitation, as is discussed in the article by Schmidt, Earley and Friedel [7]. This may result in the formation of channels in the rock, through which the leaching fluid flows preferentially. A linearized analysis of the channelling instability in the context of upwelling melt in the Earth's mantle has been presented by Aharonov, Whitehead, Kelemen and Spiegelman [8], and it is possible that a similar analysis may be relevant here also.

In this paper, we address the simple question of where the leaching liquor goes after it has been injected into the rock, and how it may be possible to recover all the liquor. Thus we ignore the effect of chemical reactions, of the type considered in the models by Lapidus [9] and Dewynne, Fowler and Hagan [10], for example. In addition, the dynamical changes to the rock properties caused by these reactions [7] are also ignored, and for simplicity, we assume that the rock properties are homogeneous; thus, no strata, fissures or faults are considered here.

In a practical large-scale field mineral leaching operation, the geometry of the groundwater flow is likely to be highly three-dimensional, since it is the usual practice to lay out a staggered grid pattern of alternate injection and production wells drilled from the surface, as indicated by Bartlett [1]. Indeed, Forbes [11] suggested that complete recovery of the leaching liquor may be possible in such a practical three-dimensional situation, by drilling spatially periodic wells, and arranging the geometry so that recovery occurred at points directly below the acid injection points. Furthermore, water would be injected below the recovery points, to prevent any acid escaping down further into the rock. In practice, the injection of acid, the recovery of liquor and the injection of water at each of the wells could be achieved by a system of three concentric pipes.

The purpose of the present paper is to examine a somewhat simpler geometry than that suggested by Forbes [11], as a test of whether such a mineral leaching scheme might actually achieve its objective of complete acid recovery. For this reason, we study here a two-dimensional leaching situation, in which the injection and extraction wells are equivalent to long horizontal perforated pipes. This is obviously a mathematical simplification of the situation of greatest interest, but it is by no means lacking in practical interest. Indeed, Bartlett [1] indicates that new drilling technology, developed in the first instance for use in the petroleum industry, has made horizontal wells possible, and there may be situations where this is the preferred method of leaching a particular mineral deposit. In addition, a two-dimensional geometry is possibly a good model for the case in which horizontal wells are drilled into the rock, from the side wall of an old mine tunnel; exactly this situation was trialled experimentally at Mount Isa, in the far north of Australia.

Under these idealizations, the flow through the rock may be assumed to be governed by Darcy's law. In addition, the problem will be taken to be steady, in view of the long times required for practical leaching operations (these can be of the order of years [7]). It will be assumed that the rock is dry, so that the pore pressure of fluid within it is normally zero, and that injected fluid therefore forms a sharp boundary in the rock, that separates a fully saturated zone from a totally dry region. Again, this is an idealization of reality, but in practice it is unlikely to cause major error, particularly if the partially saturated region is confined to a relatively narrow boundary layer at the edge of the wetted region of rock.

The use of Darcy's law to model groundwater flow is well established, and its application in the petroleum industry is discussed by Hubbert [12], for example. Complex-variable techniques for two-dimensional groundwater problems, of the type considered in this paper, are outlined in the text by Verruijt [13] and presented in detail by Strack [14], who also gives an introduction to boundary-element methods. Flow in the neighbourhood of sources and sinks is discussed by Bear [15, page 319].

Recently, there has been considerable interest in applying complex-variable and boundary-integral techniques to solving free-boundary flow problems that arise in the petroleum industry. An important problem in this field is the interaction between layers of subterranean oil and water, leading to the formation of 'water cones' in some situations, when the oil is extracted. Problems of this type were originally formulated in the classical book by Muskat [16]. Lucas, Blake and Kucera [17] have studied the water-coning problem in an oil reservoir of infinite lateral extent. They modelled the extraction point as a mathematical sink, and assumed that Darcy's law held in both the water and the oil layers. These assumptions were discussed in detail by these authors, and further references may be obtained from their paper. Their work was later generalized by Lucas and Kucera [18] to account for water coning at multiple extraction wells. In two-dimensional flow, Zhang and Hocking [19] and Zhang, Hocking and Barry [20] have studied withdrawal from a vertically confined oil layer through a horizontal line sink, using conformal mapping and boundary-integral techniques, and found a limiting profile with a vertical cusp at the interface, analogous to the cone that is formed in three-dimensional flow. Their work has been generalized to the three-dimensional case by Zhang and Hocking [21].

In this paper, we investigate the situation in which the injected leaching acid in the rock is supported by a region into which water has been pumped. An additional practical difficulty, therefore, is the possibility that the interface between the two fluids may become unstable, resulting in the formation of 'fingers'. A situation of this type has been discussed by Tan and Homsy [22], and Butts and Jensen [23] give experimental verification of fingering in oil penetrating heterogeneous sand. This complicated effect is ignored in the present model, since the rock is taken here to be homogeneous; in addition, it must be assumed that the density of the mineral-bearing leaching fluid is not too greatly different from that of the supporting water.

The model equations appropriate for this situation are outlined in Section 2. We have found that the most efficient method for solving these equations is by making use of a boundary integral approach, following Martinez and Mctigue [24], Forbes, Watts and Chandler [25] and Forbes [11], and this formulation is given in Section 3. A brief outline of the numerical method used to solve this integral equation is given in Section 4, and Section 5 contains a simple but useful asymptotic approximation to the solutions. Results are shown in Section 6, and the concluding Section 7 discusses the practical use of these results.

2. The two-dimensional model

In this paper, the complete recovery of the leaching liquor is achieved by using a spatially periodic array of injection and recovery wells, similar to that sketched in Figures 1. We will begin by outlining the problem using actual dimensional variables, and then move to the use of dimensionless quantities for the remainder of the paper.

Consider a vertical arrangement of injection and extraction points. Acid is injected into the rock, a distance H below the ground. At some distance L below this point is a recovery well, at which fluid is pumped back up to the surface. Below this recovery site is a third point at which water is injected; this occurs at a distance D below the recovery point, which is a total depth $H + L + D$ below ground. Now suppose that this entire structure, of three wells arranged vertically, is translated sideways by some distance $2S$ both to the left and to the right. This pattern is repeated so that the structure is periodic in the horizontal direction, with period $2S$, and a schematic illustration of the situation is given in Figure 1(a).

By virtue of its periodicity, the problem is equivalent to a single vertical array of injection and extraction points, with effective impermeable boundaries at $x = S$ and $x = -S$. Each acid injection point (at $y = -H$) creates a volume flux Q_A of leaching acid per unit width, and the recovery points (at depth $y = -H - L$) remove a volume Q_R per unit width per unit time. Beneath these points, at the depth $y = -H - L - D$, water is injected at the volume rate Q_W per width of rock, as indicated in Figure 1(a).

According to Darcy's law, the percolation velocity $\mathbf{q}$ of fluid through the rock is given by the formula

$$\mathbf{q} = -C\nabla\big(p + \rho g y\big), \tag{1}$$

where p is the pore pressure of fluid in the rock and ρ is its density. The downward acceleration of gravity is g, and C is the usual Darcy constant, which is the rock permeability divided by the viscosity of the fluid.

Far below the injection and recovery points, where $y \to -\infty$, the pore pressure p of fluid in the rock drops to zero, so that there is a steady outflow of fluid from the system, with speed $\rho g C$ downwards through the rock. Since there is no fluid flow across the effective boundaries at $x = \pm S$, by virtue of the periodicity of the leaching arrangement, then it follows from conservation of mass that

$$Q_R + (\rho g C)(2S) = Q_A + Q_W. \tag{2}$$

We are now ready to move to the use of dimensionless variables, and these will be retained for the rest of this paper. The unit of length is chosen to be the depth H of the acid injection point below ground, and pressure is referred to the quantity Q_A/C. It turns out that the problem depends on the six dimensionless parameter groups

$$\sigma = \frac{S}{H} \quad F = \frac{Q_A}{\rho g H C} \quad \lambda = \frac{L}{H} \quad \delta = \frac{D}{H} \quad \gamma = \frac{Q_R}{Q_A} \quad \alpha = \frac{Q_W}{Q_A},$$

in which the ratio σ is obviously the dimensionless half-width of one of the periodic cells in the x-direction, as is illustrated in Figure 1(b). The second parameter F may be thought of as a dimensionless injection rate for the leaching acid. From a purely mathematical point of view, it would be possible to scale this parameter out of the problem formulation altogether,

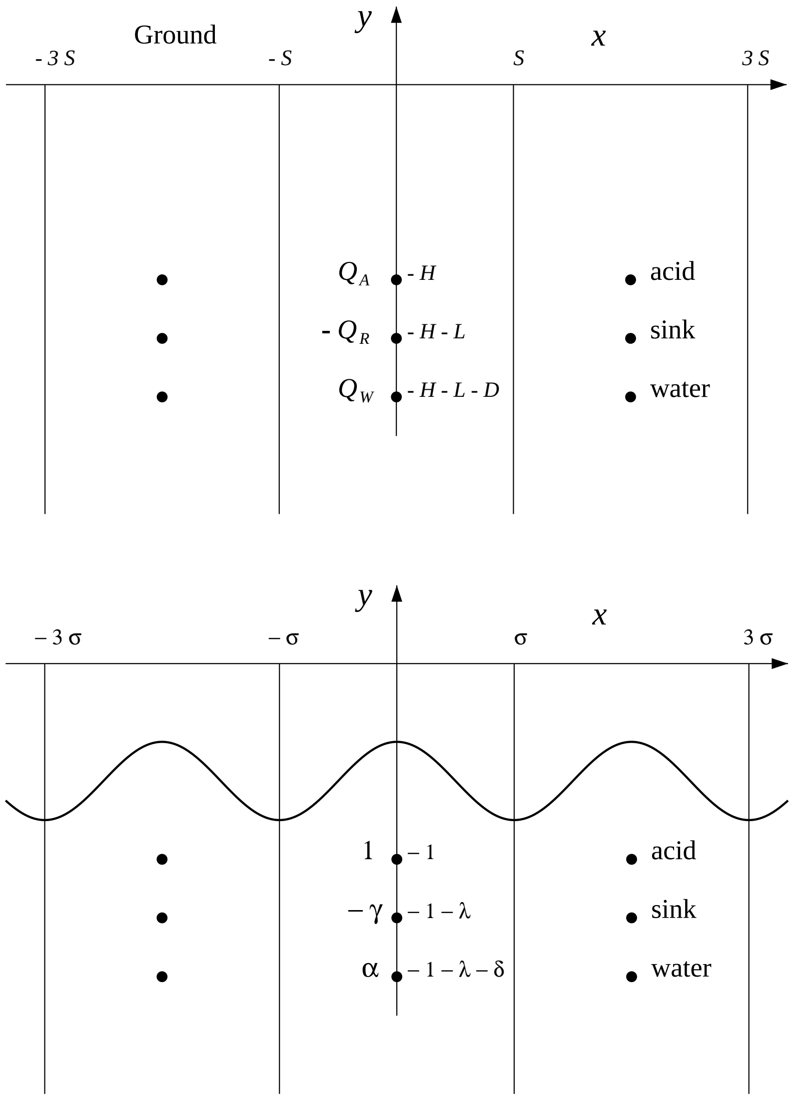

Figure 1. (a) A schematic diagram of the two dimensional spatially periodic mineral leaching flow field in dimensional coordinates, and (b) The non-dimensionalized problem.

since the depth H has not been specified explicitly. Nevertheless, we have chosen to retain the parameter F here, following Forbes, Watts and Chandler [25] and Forbes [11], since it involves the actual immersion depth H of the acid injection source, and should therefore be a quantity of immediate interest to a site engineer. The constants λ and δ are respectively the dimensionless depths of the recovery point below the acid injection point, and the further distance below this point at which the water is injected, and these quantities are likewise indicated in the dimensionless sketch of Figure 1(b). The ratio α measures the pumping rate of water into the rock to support the acid plume, and γ is the volume rate (per unit width) of the total fluid (acid plus water) that must be removed from each periodic cell. In fact, from Equation (2), this recovery rate γ is given by the formula

$$\gamma = 1 + \alpha - \frac{2\sigma}{F} \tag{3}$$

in dimensionless variables.

Darcy's law (1) now takes the form

$$\mathbf{q} = -\nabla\Phi, \tag{4a}$$

where it is convenient to define the total pressure to be

$$\Phi = p + \frac{y}{F}, \tag{4b}$$

which is made up of the fluid pore pressure p plus the hydrostatic component y/F. In the wetted region of rock, the fluid is effectively incompressible, since the rock is completely saturated in this region. Therefore, the divergence of the velocity vector $\mathbf{q}$ is zero, and Equation (4) then leads to Laplace's equation

$$\nabla^2\Phi = 0 \tag{5}$$

within the saturated region. Deep within the rock, the pore pressure p falls to zero, so that the condition

$$\Phi \to \frac{y}{F} \quad \text{as} \quad y \to -\infty \tag{6}$$

applies there. The periodicity of the leaching arrangement in the x-direction allows us to consider only the portion of rock in the region $-\sigma < x < \sigma$, and the impermeability of these boundaries to fluid flow leads to the conditions

$$\frac{\partial\Phi}{\partial x} = 0 \quad \text{on} \quad x = \pm\sigma. \tag{7}$$

Suppose that the interface between the wetted and dry rock is represented by the equation $y = \zeta(x)$. The location of this interface is unknown, and so must be found as part of the solution process. Indeed, it will be seen that, from a mathematical point of view, the determination of this interface location is the main task to be accomplished, and that once the interface has been found, all the other quantities of interest can then be obtained. On this interface, the pore pressure p of fluid in the rock falls to zero, so that

$$\Phi = \frac{y}{F} \quad \text{on} \quad y = \zeta(x), \tag{8}$$

and this is therefore the dynamical condition to be satisfied on this unknown surface location. There is also the kinematic condition

$$\frac{\partial\Phi}{\partial n} = 0 \quad \text{on} \quad y = \zeta(x), \tag{9}$$

which expresses the fact that the fluid cannot cross this boundary. Here, the symbol $\mathbf{n}$ denotes the unit vector normal to the interface and pointing out of the fluid inundated region of rock. It is important to observe that, although the boundary conditions (8) and (9) are linear, the overall problem is nonetheless nonlinear, since Laplace's equation (5) must be solved in a region that is not known in advance.

Near the injection point for acid, the fluid velocity vector **q** behaves as a line source of unit strength. By Equation (4a), the total pressure potential in Equation (4b) therefore has the form

$$\Phi \to -\frac{1}{2\pi}\log\sqrt{x^2+(y+1)^2} \quad \text{as} \quad (x, y) \to (0, -1). \tag{10a}$$

Similarly, the recovery point behaves like a line sink of strength γ given by the conservation condition (3), so that

$$\Phi \to \frac{\gamma}{2\pi}\log\sqrt{x^2+(y+1+\lambda)^2} \quad \text{as} \quad (x, y) \to (0, -1-\lambda). \tag{10b}$$

Finally, the water balloon which is injected at depth $1+\lambda+\delta$ below the ground produces a volume flux α per unit width, and so the pressure potential behaves as

$$\Phi \to -\frac{\alpha}{2\pi}\log\sqrt{x^2+(y+1+\lambda+\delta)^2} \quad \text{as} \quad (x, y) \to (0, -1-\lambda-\delta) \tag{10c}$$

near this point.

3. The boundary-integral formulation

The problem of solving Laplace's Equation (5) throughout the wetted region, subject to the boundary condition (6) far below and the effective wall conditions (7) at $x = \pm\sigma$, is most efficiently accomplished by making use of an integral equation method. To this end, we first need to obtain a Green function suitable for the present geometry. This is equivalent to finding the potential for a line source at an arbitrary point between two parallel walls, and can be solved using conformal mapping, in a generalization of the result presented by Milne-Thomson [26, page 284]. Suppose that the source between the walls has the arbitrary position (x_P, y_P), and let the field point (x_Q, y_Q) be some point in the wetted region at which the effect of the source is measured. After some algebra, we obtain the Green function in the form

$$\begin{aligned} G(P; Q) &\\ = \frac{y_P+y_Q}{4\sigma} &\\ -\frac{1}{4\pi}\log&\left[\exp\left(\frac{\pi y_P}{\sigma}\right)+\exp\left(\frac{\pi y_Q}{\sigma}\right)-2\exp\left(\frac{\pi(y_P+y_Q)}{2\sigma}\right)\cos\left(\frac{\pi(x_P-x_Q)}{2\sigma}\right)\right] \\ -\frac{1}{4\pi}\log&\left[\exp\left(\frac{\pi y_P}{\sigma}\right)+\exp\left(\frac{\pi y_Q}{\sigma}\right)+2\exp\left(\frac{\pi(y_P+y_Q)}{2\sigma}\right)\cos\left(\frac{\pi(x_P+x_Q)}{2\sigma}\right)\right]. \end{aligned} \tag{11}$$

This function is symmetric with respect to the points P and Q; that is, $G(P; Q) = G(Q; P)$. In addition, it obeys the effective wall conditions (7). It satisfies Laplace's Equation (5) at all points (x_Q, y_Q), except at the source point (x_P, y_P) where the function can be shown to have the limiting form

$$G(P; Q) \to -\frac{1}{2\pi}\log\sqrt{(x_P-x_Q)^2+(y_P-y_Q)^2} \quad \text{as} \quad P \to Q, \tag{12}$$

as expected. Finally, if the source point P is allowed to sink far down into the rock, then it is straightforward to show that

$$G(P;Q) \to \frac{y_P - y_Q}{4\sigma} \quad \text{as} \quad y_P \to -\infty. \tag{13}$$

The Green function in Equation (11) can now be used to construct an integral equation formulation for the solution of this problem, through the use of Green's second formula

$$\int\int_S \left[\Phi(P) \frac{\partial G(P;Q)}{\partial n_P} - G(P;Q) \frac{\partial \Phi(P)}{\partial n_P} \right] \mathrm{d}S_P = 0. \tag{14}$$

This equation is applied over a volume of some width W in the z-direction (perpendicular to the plane shown in Figure 1(b)). The closed surface S of this volume consists of the planes $x = \pm\sigma$ and $z = 0$ and $z = W$ and the unknown surface $y = \zeta(x)$, along with some surface infinitely deep within the rock. In addition, the three injection or extraction points, at $y = -1$, $y = -1 - \lambda$ and $y = -1 - \lambda - \delta$, are excluded by cylindrical surfaces of width W, and the point Q on the free surface is likewise excluded by a half-cylindrical surface. (Notice that, if the Green function in Equation (14) is chosen simply to be the number 1, then the mass conservation condition (3) is recovered).

The contribution to the integrals in Equation (14) from the side surfaces is zero, since both the pressure potential Φ and the Green function G in Equation (11) satisfy the effective wall conditions (7). Deep within the rock, the total pressure satisfies the limiting relation (6), and the equivalent condition for the Green function is given by Equation (13), and thus the contribution to Equation (14) from this surface is $-(y_Q W)/(2F)$. Here, $y_Q = \zeta(x_Q)$ is the point on the surface. The half-cylindrical surface which excludes this surface point Q from the volume may be shown to contribute a term $W\Phi(Q)/2$ to the integral, by virtue of the condition (12) that is satisfied by the Green function as point P approaches point Q.

Finally, the three singular points that represent the injection and extraction of fluid in the rock may be shown to contribute to the integral in Equation (14). The acid source, at the point $(0, -1)$, gives a term $-WG(0, -1; Q)$ when the cylindrical surface excluding it from the volume is allowed to shrink to zero radius about the line source. Similarly, the extraction point at $y = -1 - \lambda$ contributes

$$\gamma W G(0, -1 - \lambda; Q)$$

and the water injection point at $(0, -1 - \lambda - \delta)$ adds

$$-\alpha W G(0, -1 - \lambda - \delta; Q)$$

to the integral.

When all these contributions are written out in full, and the width W of the test volume is cancelled from the equation, Green's second formula (14) yields

$$\begin{aligned} &\tfrac{1}{2}\Phi(Q) - \frac{y_Q}{2F} - G(0, -1; Q) + \gamma G(0, -1 - \lambda; Q) \\ &\quad -\alpha G(0, -1 - \lambda - \delta; Q) + \mathrm{CPV} \int_{-\sigma}^{\sigma} \Phi(P) \frac{\partial G(P;Q)}{\partial n_P} \frac{\mathrm{d}\ell_P}{\mathrm{d}x_P} \, \mathrm{d}x_P = 0. \end{aligned} \tag{15}$$

In this equation, the integral is now taken over the unknown interface $y_P = \zeta(x_P)$. In fact, since the point Q is also on the interface, the integrand is singular at $P = Q$, so that a Cauchy principal value interpretation is needed for the integral, and this is denoted by the letters 'CPV' appearing in this equation. The outward-pointing normal to the surface is denoted $\mathbf{n}$, and the element of length along the surface is

$$\mathrm{d}\ell_P = \sqrt{\left(\mathrm{d}x_P\right)^2 + \left(\mathrm{d}y_P\right)^2}.$$

Notice that the kinematic condition (9) of no flow normal to the interface has already been used in Equation (15). This equation is an extension and generalization of the result presented by Strack [14], for example.

The function Φ at the interface may be replaced by y/F, by virtue of the dynamic condition (8), and so Equation (15) becomes a relation involving only the unknown interface shape $y = \zeta(x)$. The interface is symmetric about $x = 0$, so that the condition

$$\zeta(-x) = \zeta(x) \tag{16}$$

holds, and after a little algebra, the relation (15) takes the form

$$\begin{aligned} &-G(0,-1;Q) + \gamma G(0,-1-\lambda;Q) - \alpha G(0,-1-\lambda-\delta;Q) \\ &\quad + \frac{1}{F}\mathrm{CPV}\int_0^{\sigma} \zeta_P \left[\zeta_P' \frac{\partial G}{\partial x_P}(-x_P,\zeta_P;x_Q,\zeta_Q) + \frac{\partial G}{\partial y_P}(-x_P,\zeta_P;x_Q,\zeta_Q) \right. \\ &\qquad\qquad \left. - \zeta_P' \frac{\partial G}{\partial x_P}(x_P,\zeta_P;x_Q,\zeta_Q) + \frac{\partial G}{\partial y_P}(x_P,\zeta_P;x_Q,\zeta_Q) \right] \mathrm{d}x_P = 0. \end{aligned} \tag{17}$$

This is the integral equation that must be solved to find the location of the interface between the wetted and dry portions of the rock. At the point $x = 0$, the symmetry condition (16) indicates that the interface must be flat, and at the other end of the domain of integration, where $x = \sigma$, a fluid stagnation point is expected. From Darcy's law (4a) therefore, $\mathbf{q} = \mathbf{0}$ at this point, and then the interface condition (9) shows that the surface must be flat here also. Therefore, we impose the additional two conditions

$$\zeta'(x) = 0 \quad \text{at } x = 0, \sigma. \tag{18}$$

Equations (17) and (18) constitute the integral equation formulation of this problem.

4. Numerical solution

This Section outlines the numerical method used in the solution of the boundary integral formulation of the problem. Such methods have become somewhat standard in recent years in the solution of steady free-boundary problems, and so a brief description of the technique is all that is required here.

The interval $0 \leqslant x \leqslant \sigma$ over which the interface is to be sought is first discretized into $N-1$ sub-intervals, represented by the points $x_1, x_2, \ldots, x_N$. Clearly $x_1 = 0$ and $x_N = \sigma$. The unknown interface is represented by the N discrete point values $\zeta_1, \zeta_2, \ldots, \zeta_N$ at these numerical grid points. The numerical method seeks to solve for an $(N-1)$-vector of unknowns

$$\mathbf{u} = [\zeta_1; \zeta_2', \ldots, \zeta_{N-1}']^T,$$

and an initial guess is made for these quantities, to begin the iterative solution process. (Notice that the elevation itself is sought at the first point, but the slopes are to be determined at the remaining $N-2$ mesh points). The conditions $\zeta_1' = 0$ and $\zeta_N' = 0$ are specified, in accordance with Equations (18).

On the basis of the initial guess made for the vector $\mathbf{u}$ of unknowns, the interface shape is constructed using trapezoidal-rule integration in the form

$$\zeta_{j+1} = \zeta_j + \tfrac{1}{2}\Delta x\left[\zeta_j' + \zeta_{j+1}'\right] \qquad j = 1, 2, \ldots, N-1.$$

The integral equation (17) is evaluated at the $N-1$ half-mesh points $x_{j+1/2} = (x_j + x_{j+1})/2$ using composite trapezoidal rule integration. Because the Cauchy singular point $P = Q$ is located at the whole mesh points, it may simply be ignored, by symmetry. This equation gives rise to a system of $N-1$ algebraic equations, which may be written in the vector form $\mathbf{E}(\mathbf{u}) = \mathbf{0}$, and a damped Newton's method strategy is used to solve this system by iteratively updating the guess for the vector $\mathbf{u}$.

5. Asymptotic approximation

It is of benefit to discuss a simple approximate solution to this problem, and this is the topic of this Section. The solution is of use both as a starting guess for the numerical method of Section 4, and as a means of developing some simple but practical inequalities that guide the operation of this leaching strategy.

If the effective walls at $x = \pm\sigma$ are quite close together, then σ/F is a small quantity and it is to be expected that the interface would be nearly flat, at some location $y = Y_0$. In that case, the solution for the total pressure potential Φ can be written down at once, using the Green function (11) and the method of images.

For a flat interface at the location $y = Y_0$, the acid injection point $(0, -1)$ has an image point at $(0, 2Y_0 + 1)$. Similarly, the recovery point and the water injection point have images at $(0, 2Y_0 + 1 + \lambda)$ and $(0, 2Y_0 + 1 + \lambda + \delta)$ respectively. The solution for the total pressure Φ in the region $y < Y_0$ is therefore

$$\begin{aligned}\Phi(x_Q, y_Q) \;=\; & \frac{Y_0}{F} + \left[G(0, -1; x_Q, y_Q) + G(0, 2Y_0 + 1; x_Q, y_Q)\right] \\ & -\gamma\left[G(0, -1-\lambda; x_Q, y_Q) + G(0, 2Y_0 + 1 + \lambda; x_Q, y_Q)\right] \\ & +\alpha\left[G(0, -1-\lambda-\delta; x_Q, y_Q) + G(0, 2Y_0 + 1 + \lambda + \delta; x_Q, y_Q)\right]. \qquad (19)\end{aligned}$$

It may be shown that the three limiting conditions (10a,b,c) are satisfied by this solution (19), which also fulfils the requirement (8) deep within the rock as $y_Q \to -\infty$. In addition, a certain amount of algebraic manipulation shows that the approximate solution (19) satisfies the Neumann condition $\partial\Phi/\partial y_Q = 0$ on the line $y_Q = Y_0$, and this is the equivalent of the kinematic condition (9) to this order of approximation.

It remains to satisfy the dynamic interface condition $p = 0$ expressed by Equation (8). At this order of approximation, the appropriate condition is

$$\Phi(0, Y_0) = \frac{Y_0}{F}, \qquad (20a)$$

in which

$$\begin{aligned}\Phi(0, Y_0) \;=\; & \frac{Y_0}{F} + \big[G(0, -1; 0, Y_0) + G(0, 2Y_0 + 1; 0, Y_0)\big] \\ & -\gamma\big[G(0, -1 - \lambda; 0, Y_0) + G(0, 2Y_0 + 1 + \lambda; 0, Y_0)\big] \\ & +\alpha\big[G(0, -1 - \lambda - \delta; 0, Y_0) + G(0, 2Y_0 + 1 + \lambda + \delta; 0, Y_0)\big]. \qquad (20b)\end{aligned}$$

After some algebra, it may be shown that this relation (20) gives rise to a transcendental equation for the interface height $y_Q = Y_0$. This condition is

$$\begin{aligned}& \frac{Y_0 - 1}{F} + \frac{\gamma\lambda - \alpha\lambda - \alpha\delta}{2\sigma} - \frac{1}{\pi}\log\Big|\exp\big(-\pi/\sigma\big) - \exp\big(\pi Y_0/\sigma\big)\Big| \\ & \quad + \frac{\gamma}{\pi}\log\Big|\exp\big(-\pi(1+\lambda)/\sigma\big) - \exp\big(\pi Y_0/\sigma\big)\Big| \\ & \quad - \frac{\alpha}{\pi}\log\Big|\exp\big(-\pi(1+\lambda+\delta)/\sigma\big) - \exp\big(\pi Y_0/\sigma\big)\Big| = 0. \qquad (21)\end{aligned}$$

This is a complicated expression for the height Y_0 of the interface, but it can be solved easily enough numerically, and we use Newton's method for this purpose. In this way, Equation (21) serves as a valuable check on the numerical accuracy of the solutions obtained by the full scheme outlined in Section 4, and has acted as a guide for the number N of numerical grid points needed to obtain solutions to a required degree of accuracy.

The approximation (21) also serves as a useful guide for the parameter regions in which solutions of the type we are seeking are likely to be found. Since the stagnation point at $(0, Y_0)$ must lie above the acid injection point at $y = -1$, then $Y_0 > -1$, and so it follows that $\exp(\pi Y_0/\sigma) > \exp(-\pi/\sigma)$. Therefore, if we make the approximation

$$\exp(\pi Y_0/\sigma) - \exp(-\pi/\sigma) \approx \exp(\pi Y_0/\sigma)$$

in Equation (21), with similar approximations in the other two logarithmic terms, then we are led to the simple result that

$$Y_0 \approx -1 + \frac{(1 - 2\sigma/F)\lambda - \alpha\delta}{2\sigma/F}. \qquad (22)$$

In many instances, the simplified result (22) is actually a close approximation to the value of Y_0 obtained numerically from the transcendental Equation (21), but more importantly, it leads to some very useful inequalities.

As the interface lies above the acid injection point, then $Y_0 > -1$, and the simplified formula (22) at once suggests the requirement

$$\frac{1}{\alpha}\left(1 - \frac{2\sigma}{F}\right) > \frac{\delta}{\lambda}. \qquad (23)$$

Furthermore, for the inequality (23) to be realized at all, it is necessary to impose the extra condition

$$\sigma < \frac{F}{2}. \qquad (24)$$

These two inequalities (23) and (24) have proven to be extraordinarily useful in choosing parameter values for this study, and our experience is that the full numerical method of Section 4 will only converge to a solution when these two inequalities are satisfied.

6. Presentation of results

We begin this Section with an example of a flow field that strongly satisfies the main objective of this study, which is to produce a solution for which rock is leached but none of the introduced acid escapes into the rock. A cross-section of a portion of such a flow field is presented in Figure 2. In this diagram, as for the rest of this paper, the parameter F has been fixed at the value $F = 0{\cdot}1$. As explained in Section 2, this is not an important parameter from a purely mathematical point of view, since it can be scaled out of the problem altogether. Physically, however, it retains significance as a means of defining length scales in an *in situ* leaching experiment, and the value $F = 0{\cdot}1$ corresponds approximately to an injection depth of 2 kilometres, at a seepage rate of about 1 centimetre per day deep within the wetted rock, and an injection rate for acid of about 1 litre per minute per metre width.

Figure 2 shows a portion of the rock in the interval $0 < x < \sigma$, for the case $\sigma = 0{\cdot}01$. The parameters λ and δ have the values $\lambda = 0{\cdot}02$ and $\delta = 0{\cdot}01$, which means that the leaching acid is injected at the point $y = -1$ at the left of this figure, the fluid recovery occurs at the point $y = -1{\cdot}02$ and the water is injected at the point where $y = -1{\cdot}03$. The volume injection rate of water per width is $\alpha = 1{\cdot}4$, so that 40% more water is being injected than leaching acid. This then forces the volume withdrawal rate of fluid per width, at the point $(0, -1 - \lambda)$,

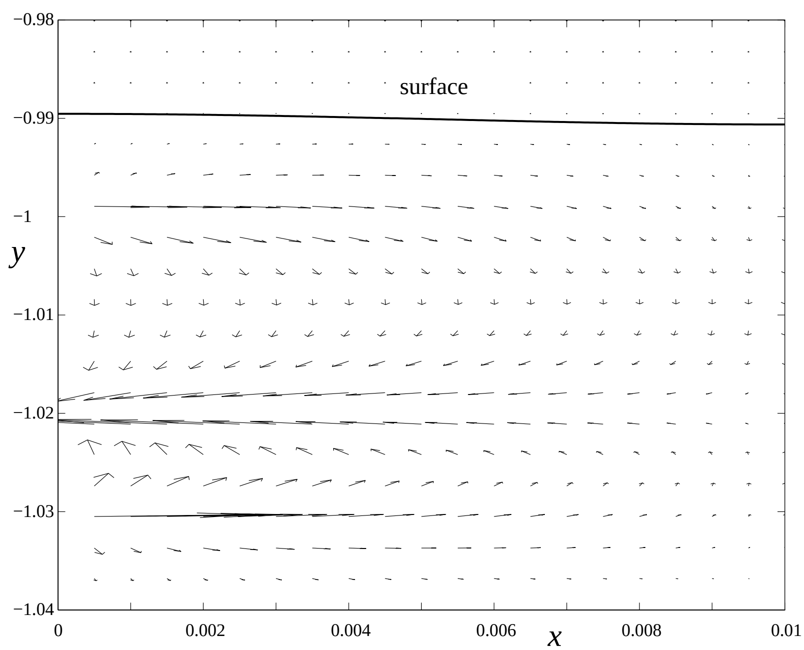

Figure 2. A portion of a computed flow field for $0 < x < \sigma$, with parameter values $F = 0{\cdot}1$, $\sigma = 0{\cdot}01$, $\lambda = 0{\cdot}02$, $\delta = 0{\cdot}01$ and water injection rate $\alpha = 1{\cdot}4$. The surface of the wetted region of rock is also shown.

to be $\gamma = 2{\cdot}2$, as indicated by Equation (3). There were $N = 241$ numerical grid points used in this solution, and the stagnation point above the acid source is computed to occur at height $y = -0{\cdot}9895$. From the asymptotic solution (21), the approximate interface height is computed to be $Y_0 = -0{\cdot}9890$, which shows that agreement between these two values is extremely good, even for this large water injection rate $\alpha = 1{\cdot}4$, which as will be seen later, is close to a maximum permissible value.

The interface is shown in Figure 2 for this case, and was obtained using the numerical method of Section 4. Once this interface has been obtained, it is then straightforward to compute the total pressure Φ at any desired point within the rock. We follow essentially the same procedure that led to the development of Equation (15), except that now the point Q is internal rather than being on the wetted surface, and so it is excluded from the volume in Equation (14) by a full cylindrical surface, which gives a contribution $W\Phi(Q)$ to that equation. Thus, for any internal point Q, the pressure is obtained from the formula

$$\begin{aligned}\Phi(Q) \;=\; & \frac{y_Q}{2F} + G(0,-1;Q) - \gamma G(0,-1-\lambda;Q) + \alpha G(0,-1-\lambda-\delta;Q) \\ & -\frac{1}{F}\int_0^{\sigma} \zeta_P \left[\zeta_P' \frac{\partial G}{\partial x_P}(-x_P,\zeta_P;x_Q,y_Q) + \frac{\partial G}{\partial y_P}(-x_P,\zeta_P;x_Q,y_Q)\right. \\ & \left. -\zeta_P' \frac{\partial G}{\partial x_P}(x_P,\zeta_P;x_Q,y_Q) + \frac{\partial G}{\partial y_P}(x_P,\zeta_P;x_Q,y_Q)\right] \mathrm{d}x_P. \qquad (25)\end{aligned}$$

Fluid seepage velocities in the x- and y-directions have been computed by straightforward finite-difference approximations to the x-and y-derivatives of the pressure computed from Equation (25), according to Darcy's law (4a).

The fluid velocity vectors are shown in Figure 2 as small arrows. It is clear that the acid injected at the point $(0, -1)$ floods a volume of rock before it is all pumped out at the extraction point $(0, -1{\cdot}02)$. Some of the water injected at $(0, -1{\cdot}03)$ is also withdrawn at the extraction point, while the rest of it escapes away deep into the rock. Thus the water injected at the point $(0, -1-\lambda-\delta)$ does indeed act to block the acid moving down below the extraction point and escaping. This point is amplified in the following discussion, by presenting results for the pressure and vertical velocity component at the edge $x = \sigma = 0{\cdot}01$ of the periodic region.

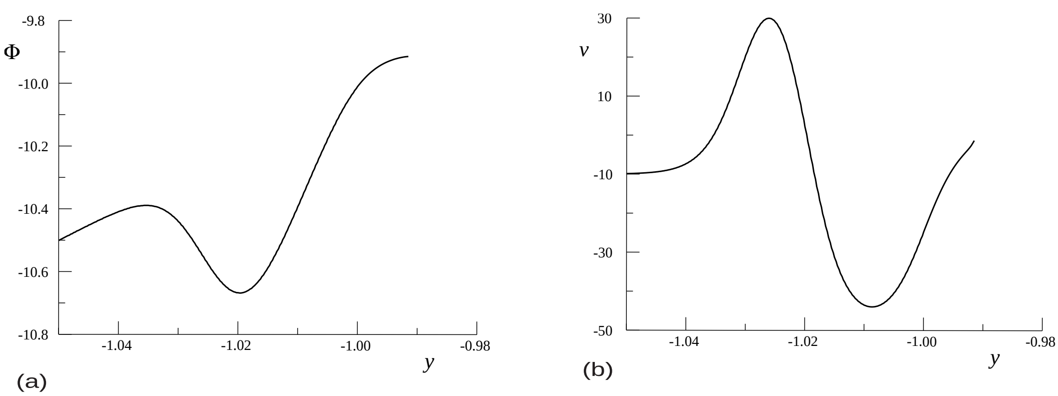

Figure 3. (a) Pressure Φ and (b) vertical velocity v at the edge $x = \sigma$ of the periodic region, as a function of depth coordinate y. Here, $F = 0{\cdot}1$, $\sigma = 0{\cdot}01$, $\lambda = 0{\cdot}02$, $\delta = 0{\cdot}01$ and $\alpha = 1{\cdot}4$.

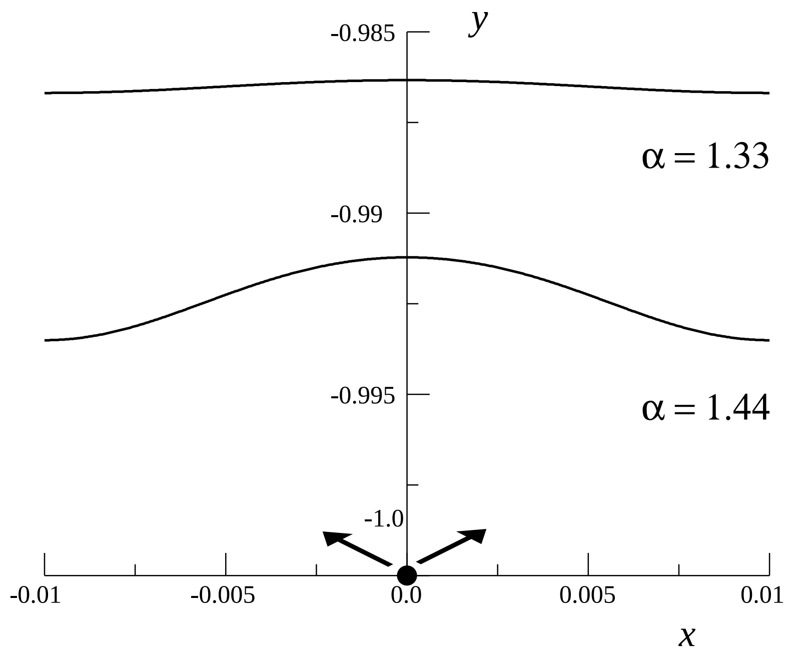

Figure 4. Two different interfaces corresponding to water injection rates of $\alpha = 1{\cdot}33$ and $\alpha = 1{\cdot}44$, for the case $F = 0{\cdot}1$, $\sigma = 0{\cdot}01$, $\lambda = 0{\cdot}02$ and $\delta = 0{\cdot}01$. The acid injection point is shown, and the scale on both axes is the same.

Figure 3(a) shows the total pressure Φ along the line $x = \sigma$ as a function of vertical coordinate y, for the same case as illustrated in Figure 2. The pressure was computed from the free surface profile using Equation (25). Superimposed on the hydrostatic component y/F of the pressure is a clear maximum at about $y = -1{\cdot}035$, and a corresponding pressure minimum at about $y = -1{\cdot}02$. These local maximum and minimum are clear evidence for the presence of stagnation points at the effective wall $x = \sigma$, and indicate that there are streamlines emanating from both the water injection point and the recovery point, and terminating at the effective wall. This confirms that the acid injected at $(0, -1)$ is blocked by the water balloon, and so prevented from escaping away into the rock.

This point is further clarified in Figure 3(b), which shows the vertical velocity component $v = -\partial\Phi/\partial y$ as a function of coordinate y, along the line $x = \sigma$ for this same case. A clear region of positive velocity v is evident in the approximate interval $-1{\cdot}035 < y < -1{\cdot}02$, and this shows that, in this interval, the injected water is moving *upwards* along the line $x = \sigma$, so preventing any downward motion of the acid.

The asymptotic solution of Section 5 is capable of giving an estimate of the location of the two stagnation points in the flow field, along the vertical lines $x = \pm\sigma$. All that is required is to compute an analytical expression for the velocity vector $\mathbf{q}$, using the Darcy law (4a) and the approximate expression (19) for the total pressure, and then to seek the points where $\mathbf{q} = \mathbf{0}$. This has been done in the Appendix, and the location of the stagnation points may be found from Equation (A7) given there. For the parameter values used in Figures 2 and 3, this formula estimates that the two stagnation points occur at the heights $y = -1{\cdot}01972$ and $y = -1{\cdot}03539$, and these values are in very good agreement with the numerical results of Figure 3(b).

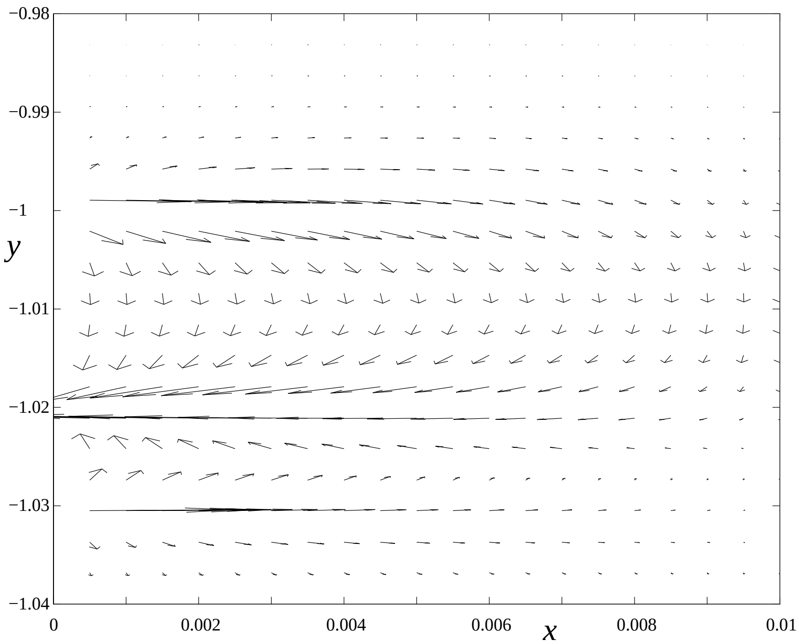

Figure 5. A portion of a computed flow field for $0 < x < \sigma$, with parameter values $F = 0{\cdot}1$, $\sigma = 0{\cdot}01$, $\lambda = 0{\cdot}02$, $\delta = 0{\cdot}01$ and water injection rate $\alpha = 0{\cdot}7$.

It turns out that there is a maximum permissible value of the water injection rate α, for fixed values of the other parameters. This seems at first counter-intuitive, but is easily explained. As the water injection rate α is increased, so the strength γ of the extraction point must also increase, since there is a fixed volume outflow permitted at infinity. Thus, increasing α results in a stronger extraction point, which draws down the interface closer to the point at which acid is injected.

This behaviour is illustrated in Figure 4. Two different interface profiles are shown for the case $\sigma = 0{\cdot}01$, $\lambda = 0{\cdot}02$ and $\delta = 0{\cdot}01$, for the two different values $\alpha = 1{\cdot}33$ and $\alpha = 1{\cdot}44$ of the water injection rate. The scale on both axes is the same, so that the interfaces are as they would actually appear. The acid injection point at $(0, -1)$ is also shown. As α is increased, the interface moves down quite strongly toward the acid injection point, and becomes more curved as it does so. Presumably the interface would eventually meet the source point at $(0, -1)$, although the numerical method of Section 4 fails to converge before this occurs, and in fact the interface shown with $\alpha = 1{\cdot}44$ is the largest value of the water injection rate that we could compute for these parameter values. In any event, an interface that actually incorporates the acid source point is unlikely to be of much practical interest, even if it is a theoretical limiting case, and so has not been pursued further here.

It is by no means the case that the only leaching strategies that recover all the leaching acid are those for which α is close to its theoretical maximum, as in Figure 2. To illustrate this point, a solution is shown in Figure 5 with only half the water input rate, $\alpha = 0{\cdot}7$. For this case, complete blocking of the acid by the water balloon still occurs, as will be seen presently, even although the water injection rate is only 70% of the acid injection rate. The free boundary is not shown in this figure, since it has moved up to the level $y = -0{\cdot}95500$. This agrees with the value Y_0 obtained from the asymptotic solution (21) to at least five decimal places, and the numerically obtained interface is flat to this same accuracy. This confirms that the numerical

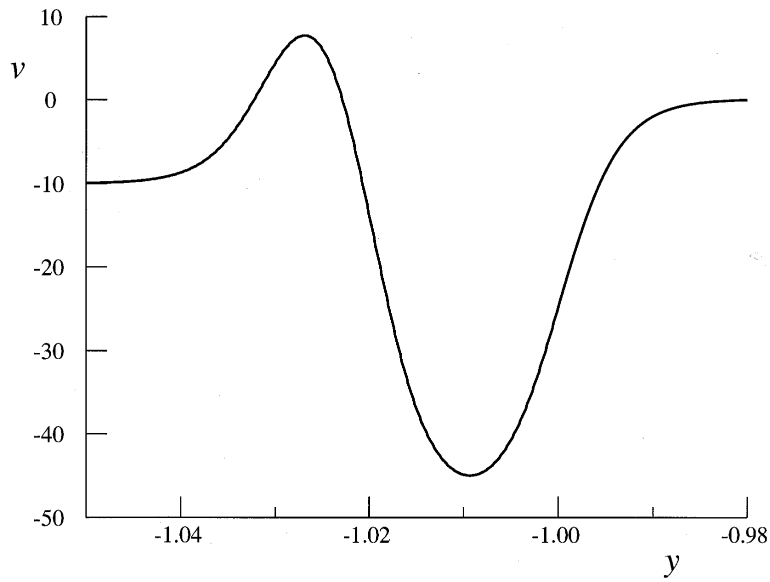

Figure 6. Vertical velocity v at the edge $x = \sigma$ of the periodic region, as a function of depth coordinate y. Here, $F = 0{\cdot}1$, $\sigma = 0{\cdot}01$, $\lambda = 0{\cdot}02$, $\delta = 0{\cdot}01$ and $\alpha = 0{\cdot}7$.

method of Section 4 is capable of very high accuracy in this problem. In all other respects, however, the solution of Figure 5 is rather similar to that shown in Figure 2, since all the acid is eventually drawn into the recovery point at $(0, -1{\cdot}02)$. Some of the water injected at $(0, -1{\cdot}03)$ is also withdrawn at the extraction point, and the rest moves down into the rock. From a practical point of view, Figure 5 with $\alpha = 0{\cdot}7$ is probably to be preferred over the flow field shown in Figure 2, since it still recovers all the acid, it leaches a larger volume of rock, and it uses much less water.

To confirm that the case $\alpha = 0{\cdot}7$ in Figure 5 does indeed block the escape of acid from the desired leaching region, the vertical velocity at $x = \sigma = 0{\cdot}01$ has been plotted in Figure 6, as a function of the depth coordinate y. This graph shows a *positive* vertical component, when y is in the approximate interval $-1{\cdot}032 < y < -1{\cdot}023$. This is therefore qualitatively similar to Figure 3(b), and once again indicates that the downward motion of the leaching acid is ultimately blocked by the upward motion of the injected water towards it, even at $x = \sigma$. The asymptotic solution of Section 5 again gives very close agreement with the numerical solution in this case; from Equation (A7) in the Appendix, we compute the location of the stagnation points to be $y = -1{\cdot}02287$ and $y = -1{\cdot}03225$.

In Figure 4 it was seen that, for fixed horizontal spacing 2σ between leaching wells, increasing the water injection rate α caused the wetted surface to drop down toward the acid injection point, and this led to one type of limiting configuration in which the interface itself presumably touches the acid source. We now investigate the situation in which the water injection rate α is kept fixed, but the distance between the wells is increased.

Four interfaces are shown in Figure 7, for the four values of the half-distance σ between wells $\sigma = 0{\cdot}01, 0{\cdot}015, 0{\cdot}02$ and $0{\cdot}025$. The other parameters have the values $\lambda = 0{\cdot}02$, $\delta = 0{\cdot}01$ and the water injection rate is fixed at the value $\alpha = 0{\cdot}7$, as in Figures 5 and 6. The scale on both axes is the same, so that the interfaces are shown as they would appear.

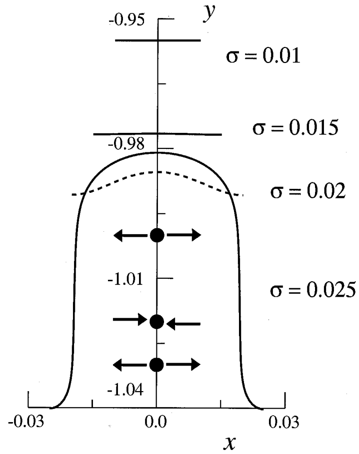

Figure 7. Four different interfaces corresponding to distances $\sigma = 0{\cdot}01$, $\sigma = 0{\cdot}015$, $\sigma = 0{\cdot}02$ and $\sigma = 0{\cdot}025$ for the case $F = 0{\cdot}1$, $\lambda = 0{\cdot}02$, $\delta = 0{\cdot}01$ and water injection rate $\alpha = 0{\cdot}7$. The scale on both axes is the same, and the acid injection point, the extraction point and the water injection point are all shown with arrows indicating the direction of flow. The interface for $\sigma = 0{\cdot}02$ has been drawn with a dotted line.

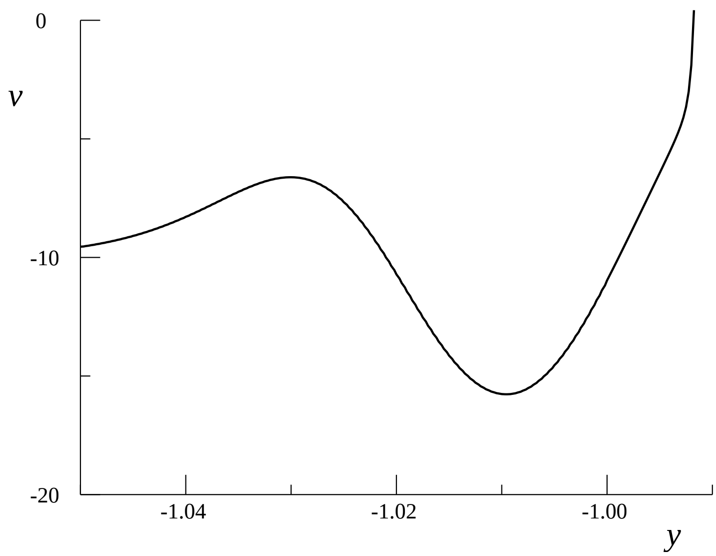

Figure 8. Vertical velocity v at the edge $x = \sigma$ of the periodic region, as a function of depth coordinate y. Here, $F = 0{\cdot}1$, $\sigma = 0{\cdot}02$, $\lambda = 0{\cdot}02$, $\delta = 0{\cdot}01$ and $\alpha = 0{\cdot}7$.

The results in Figure 7 are in accordance with physical intuition. As the well separation parameter σ is increased, the level of the interface drops, and the interface itself becomes more curved. The largest value of σ for which the numerical method of Section 4 converged was the case $\sigma = 0{\cdot}025$, and this is also shown on the diagram. In this case, the interface is very highly curved indeed, and its lowest point (at $x = \sigma$) lies below even the point at which the water balloon is injected. It seems clear that there will be a limiting value of σ, at which the point of intersection between the interface and the effective wall $x = \sigma$ falls away to infinity. If σ is increased beyond this value, then the interfaces in each periodic cell will not join up, and each well will be surrounded by its own detached vertical plume of acid and water, similar to the situation investigated by Forbes [11].

Of greater practical importance is the value of σ at which complete blocking of the acid still occurs. Of the solutions shown in Figure 7, only the case $\sigma = 0{\cdot}01$ appears to fulfil this criterion. To illustrate this, the vertical velocity component v has been shown in Figure 8 at the effective wall $x = \sigma$, for the case $\sigma = 0{\cdot}02$. Now it is clear that there is no region for which the vertical velocity is positive, and that, as a result, the water balloon cannot act to block the downward movement of acid, which must of necessity escape away to infinity. This is therefore a situation which practioners would be keen to avoid, on both economic and environmental grounds.

7. Discussion and significance

This paper has used a boundary integral method to study a strategy for two-dimensional mineral leaching, in which the overall aim has been to attempt to recover all the leaching fluid introduced into the rock. This is motivated by obvious environmental and economic factors. In practice, the two-dimensional geometry assumed here would be achieved by the use of horizontal perforated pipes with lengths that are orders of magnitude greater than their diameters. Bartlett [1] indicates that horizontal drilling is now possible, so that the assumption of two-dimensional flow may be close to the real situation in some circumstances. In addition, horizontal pipes have been used in leaching trials in Mount Isa in Queensland, Australia, by drilling in through the side walls of old mine shafts.

The central point of this investigation is that we have succeeded in our aim of injecting leaching liquors into the rock, and then recovering them completely. The strategy adopted is to use injection or extraction pipes that are spaced periodically in the horizontal direction. This effectively creates a periodic system of cells within the rock, that possess impermeable boundaries, and are therefore essentially isolated from one another. In each of these cells there is an injection point for the leaching acid, an extraction point at some distance below this, and a third point below the other two, through which a water balloon is injected. In an actual field trial, pure water could be injected instead of leaching acid in the outer two cells in the periodic array, and this should preserve the features of the present study.

Provided that the horizontal distance 2σ between the injection points is not excessive, the water balloon is capable of blocking the downward motion of the acid under gravity, and so giving complete recovery of the acid. This situation has been illustrated in Figures 2 and 5, and is also sketched diagrammatically in Figure 9, in the picture on the left labelled ‘blocking’. Some conditions under which this desirable situation may occur have been given. In Figure 9, the region inundated with leaching acid is shaded. On the other hand, if σ is too large or the injection rate α for water is insufficiently large, then complete blocking of the downward motion of the leaching acid cannot occur, and we have instead a situation like that sketched in the picture on the right of Figure 9 labelled ‘escaping’. Here, there is some fraction of the leaching acid that moves around the injected water balloon and escapes away to infinity. In such a case, the injected water does not totally block the periodic conduit, but instead forms a vertical plume.

For a situation in which the leaching fluid is injected through horizontal pipes drilled from the side wall of an existing mine shaft, the depth H below the surface may not be a particularly relevant quantity, so that the parameter F could be scaled out of the problem. In that case, the three defining parameters in the problem are the ratio of water to acid injected (α), the relative depth δ/λ, and the ratio σ/F. Useful relations between these three quantities are provided by

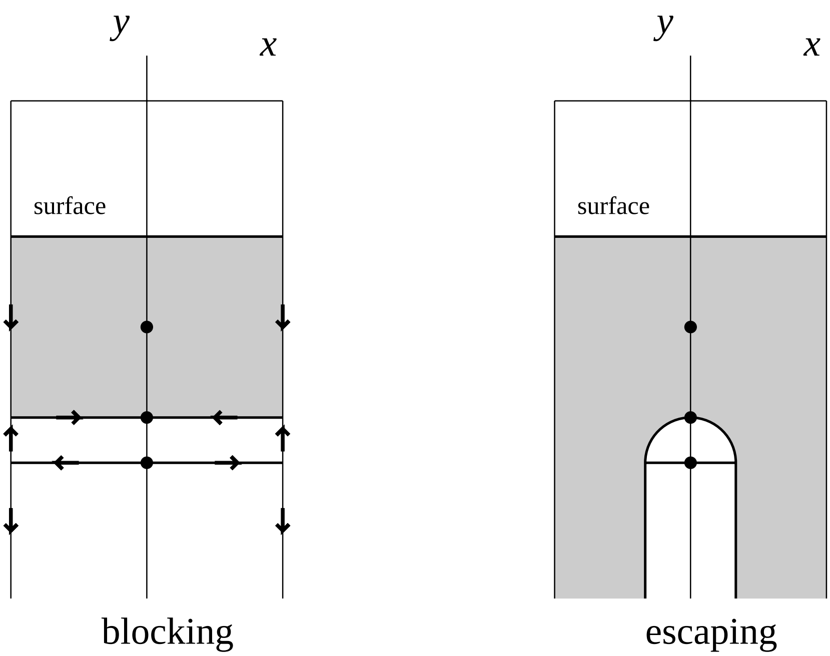

Figure 9. Two schematic diagrams of possible outcomes in the present two dimensional mineral leaching strategy, based on results of actual calculations with the present method. The picture on the left, labelled ‘blocking’, is the preferred situation of complete acid recovery. In the picture on the right, labelled ‘escaping’, the water balloon does not prevent the leaching acid from escaping away to infinity. The regions of acid are indicated by shading.

the inequalities (23) and (24), and we have indicated that practical operating conditions, with complete acid recovery, can be expected with α in the interval $0{\cdot}7 < \alpha < 1{\cdot}44$, and a depth ratio $\delta/\lambda = 0{\cdot}5$ and horizontal distance between injection points (based on acid injection rate and seepage speed) $2\sigma/F = 0{\cdot}2$, for example.

Of course, an actual geological site presents extra difficulties that have been ignored in this study. It is possible that, for a situation like the successfully blocked leaching case sketched on the left of Figure 9, the pregnant leaching liquor may form an unstable interface with the water balloon injected below it, which could give rise to interfacial fingering of the type discussed by Tan and Homsy [22]. In practice, it may be possible to overcome this problem by increasing the water injection rate α, or perhaps even by replacing the water with a fluid of greater density. In addition, we have assumed here that the rock is homogeneous in its permeability properties, and this is unlikely to be the case. The presence of significant fissures in the rock would change the solutions given in this paper substantially. It is also possible that other gradual changes in rock porosity may occur throughout the site, and these may call for more general numerical methods, such as finite differences or finite elements, to be used in the solution of the problem. Certainly, a detailed knowledge of the proposed leaching site would be necessary in order to apply the strategy with confidence.

In spite of these practical difficulties, it seems that there is considerable merit in continuing studies of this type, and these should yield results that are of practical value in the field. In particular, a generalization of this idea to three-dimensional geometry, along the lines proposed by Forbes [11], is currently under investigation, and the results of this study will appear elsewhere.

Appendix: Approximate location of stagnation points

In this appendix, we use the asymptotic theory of Section 5 to estimate the location of stagnation points in the flow, along the line $x = \sigma$. The presence of these points confirms that the downward motion of the leaching acid is blocked by the presence of the water balloon, which is the situation of most practical interest.

The asymptotic formula (19) for the total pressure Φ is differentiated with respect to y_Q to give the (negative) vertical velocity component $-v_Q = \partial\Phi/\partial y_Q$. The coordinate x_Q is then set equal to σ. It is straightforward to confirm that the horizontal velocity component is zero on this line, and after some algebra, the (negative) vertical component on $x_Q = \sigma$ becomes

$$\begin{aligned} -v_Q(\sigma, y_Q) &= \frac{1}{4\sigma}\left[\tanh\left(\frac{\pi(\eta - Y_0 - 1)}{2\sigma}\right) + \tanh\left(\frac{\pi(\eta + Y_0 + 1)}{2\sigma}\right)\right] \\ &\quad - \frac{\gamma}{4\sigma}\left[\tanh\left(\frac{\pi(\eta - Y_0 - 1 - \lambda)}{2\sigma}\right) + \tanh\left(\frac{\pi(\eta + Y_0 + 1 + \lambda)}{2\sigma}\right)\right] \\ &\quad + \frac{\alpha}{4\sigma}\left[\tanh\left(\frac{\pi(\eta - Y_0 - 1 - \lambda - \delta)}{2\sigma}\right) + \tanh\left(\frac{\pi(\eta + Y_0 + 1 + \lambda + \delta)}{2\sigma}\right)\right], \end{aligned} \tag{A1}$$

where here we have written $y_Q = Y_0 - \eta$ so as to display the anti-symmetry of the vertical velocity component about the line $y_Q = Y_0$.

For convenience, we introduce the function

$$A = (\pi\eta)/(2\sigma) \tag{A2}$$

and the three constants

$$\begin{aligned} B_1 &= \big(\pi(Y_0 + 1)\big)/(2\sigma) \\ B_2 &= \big(\pi(Y_0 + 1 + \lambda)\big)/(2\sigma) \\ B_3 &= \big(\pi(Y_0 + 1 + \lambda + \delta)\big)/(2\sigma), \end{aligned} \tag{A3}$$

and make use of the identity

$$\tanh(A + B) + \tanh(A - B) = \frac{2\sinh(2A)}{\cosh(2A) + \cosh(2B)}. \tag{A4}$$

These relations (A2)–(A4) enable Equation (A1) to be expressed in the simpler form

$$-v_Q(\sigma, y_Q) = \frac{\sinh(2A)\big[K_1\cosh^2(2A) + K_2\cosh(2A) + K_3\big]}{2\sigma\prod_{j=1}^{3}\big[\cosh(2A) + \cosh(2B_j)\big]}, \tag{A5}$$

in which we have defined the three auxiliary constants

$$\begin{aligned} K_1 &= 1 - \gamma + \alpha \\ K_2 &= (\alpha - \gamma)\cosh(2B_1) + (\alpha + 1)\cosh(2B_2) + (1 - \gamma)\cosh(2B_3) \\ K_3 &= \cosh(2B_2)\cosh(2B_3) - \gamma\cosh(2B_1)\cosh(2B_3) + \alpha\cosh(2B_1)\cosh(2B_2). \end{aligned} \tag{A6}$$

From Equation (A5), it is clear that the vertical velocity component v is an odd function of η, and has a zero when $A = 0$. This is the expected stagnation point on the interface, at (σ, Y_0). In addition, there is the possibility of a further two stagnation points, when the quadratic term in the numerator of Equation (A5) becomes zero. Thus the two stagnation points associated with the blocking of the leaching acid by the injected water balloon occur on the line $x = \sigma$ when

$$\cosh(2A) = \frac{-K_2 \pm \sqrt{K_2^2 - 4K_1K_3}}{2K_1}, \tag{A7}$$

with constants K_1, and so on, given in Equation (A6). The values of η (> 0) and hence y_Q at which the two stagnation points occur may now be computed from this formula. In principle, Equation (A7) also yields the values of the physical parameters for which the desired blocking of the acid will occur, since the argument of the square root must be positive and the entire right-hand side must be greater than one, if real solutions are to exist. In practice, however, these transcendental algebraic conditions do not appear to yield to explicit inequalities, and so each choice of parameter values must be tested separately.

Acknowledgements

This research was funded, in part, by ARC small grant A6941308 from the Australian Research Council. LKF is grateful for the opportunity to visit the Mount Isa Mines Limited mineral leaching test site in 1992.

References

1. R. W. Bartlett, *Solution Mining*. Philadelphia: Gordon and Breach (1992) 276pp.
2. J. E. Pahlman, Evaluation of the potential for in situ leach mining of domestic manganese ores. In: S. A. Swan and K. R. Coyne (eds.), *In Situ Recovery of Minerals II*. New York: Engineering Foundation (1994) 299–321.
3. S. Kubo, Development of gold ore leaching method by iodine. In: S. A. Swan and K.R. Coyne (eds.), *In Situ Recovery of Minerals II*. New York: Engineering Foundation (1994) 405–431.
4. G. Pantelis and A. I. M. Ritchie, Rate-limiting factors in dump leaching of pyritic ores. *Appl. Math. Modelling* 16 (1992) 553–560.
5. J. W. Crockett, Permitting and closure of an in situ minerals recovery operation: an attorney's perspective. In: S. A. Swan and K. R. Coyne (eds.), *In Situ Recovery of Minerals II*. New York: Engineering Foundation (1994) 21–43.
6. D. R. Tweeton, J. C. Hanson, M. J. Friedel and L. J. Dahl, Field tests of geophysical methods for monitoring the flow pattern of leach solution. In: S.A. Swan and K. R. Coyne (eds.), *In Situ Recovery of Minerals II*. New York: Engineering Foundation (1994) 179–199.
7. R. D. Schmidt, D. Earley and M. J. Friedel, Dynamic influences on hydraulic conductivity during in situ copper leaching. In: S. A. Swan and K. R. Coyne (eds.), *In Situ Recovery of Minerals II*. New York: Engineering Foundation (1994) 259–286.
8. E. Aharonov, J. A. Whitehead, P. B. Kelemen and M. Spiegelman, Channeling instability of upwelling melt in the mantle. *J. Geophys. Res.* 100, no B10 (1995) 20, 433–20, 450.
9. G. Lapidus, Mathematical modelling of metal leaching in nonporous minerals. *Chem. Eng. Sci.* 47 (1992) 1933–1941.
10. J. N. Dewynne, A. C. Fowler and P. S. Hagan, Multiple reaction fronts in the oxidation-reduction of iron-rich uranium ores. *SIAM J. Appl. Math.* 53 (1993) 971–989.
11. L. K. Forbes, Progress toward a mining strategy based on mineral leaching with secondary recovery. *Appl. Math. Modelling* 20 (1996) 16–25.

12. M. K. Hubbert, *The Theory of Ground-water Motion and Related Papers*. New York: Hafner (1969) 310pp.
13. A. Verruijt, *Theory of Groundwater Flow*. London: MacMillan (1970) 190pp.
14. O. D. L. Strack, *Groundwater Mechanics*. New Jersey: Prentice Hall (1989) 732pp.
15. J. Bear, *Dynamics of Fluids in Porous Media*. New York: American Elsevier (1972) 764pp.
16. M. Muskat, *The Physical Principles of Oil Production*. New York: McGraw-Hill (1949) 922pp.
17. S. K. Lucas, J. R. Blake and A. Kucera, A boundary-integral method applied to water coning in oil reservoirs. *J. Austral. Math. Soc. Ser. B* 32 (1991) 261–283.
18. S. K. Lucas and A. Kucera, A boundary integral method applied to the 3D water coning problem. *Phys. Fluids* 8 (1996) 3008–3022.
19. H. Zhang and G. C. Hocking, Withdrawal of layered fluid through a line sink in a porous medium. *J. Austral. Math. Soc. Ser. B* 38 (1996) 240–254.
20. H. Zhang, G. C. Hocking and D. A. Barry, An analytical solution for critical withdrawal of layered fluid through a line sink in a porous medium. *J. Austral. Math. Soc. Ser. B* 39 (1997) 271–279.
21. H. Zhang and G. C. Hocking, Axisymmetric flow in an oil reservoir of finite depth caused by a point sink above an oil-water interface. *J. Eng. Math.* 32 (1997) 365–376.
22. C.-T. Tan and G. M. Homsy, Viscous fingering with permeability heterogeneity. *Phys. Fluids A* 4 (1992) 1099–1101.
23. M. B. Butts and K. H. Jensen, Effective parameters for multiphase flow in layered soils. *J. Hydrology* 183 (1996) 101–116.
24. M. J. Martinez and D. F. Mctigue, A boundary integral method for steady flow in unsaturated porous media. *Int. J. Numer. Analytical Meth. in Geomechanics* 16 (1992) 581–601.
25. L. K. Forbes, A. M. Watts and G. A. Chandler, Flow fields associated with in situ mineral leaching. *J. Austral. Math. Soc. Ser. B* 36 (1994) 133–151.
26. L. M. Milne-Thomson, *Theoretical Hydrodynamics, 5th edition*. London: MacMillan (1968) 743pp.